2012 12th IEEE-RAS International Conference on Humanoid Robots
Nov.29-Dec.1, 2012. Business Innovation Center Osaka, Japan

Development of a Full Body Multi-Axis Soft Tactile Sensor Suit for Life Sized Humanoid Robot and an Algorithm to Detect Contact States

Iori Kumagai, Kazuya Kobayashi, Shunichi Nozawa, Yohei Kakiuchi,
Tomoaki Yoshikai, Kei Okada, Masayuki Inaba
Guraduate School of Information Science and Technology, University of Tokyo
7-3-1 Hongo, Bunkyo-ku, 113-8656 Tokyo, Japan
Email: iori, kazuya, nozawa, youhei, yoshikai, k-okada, inaba@jsk.t.u-tokyo.ac.jp

***Abstract*—Recognizing environmental contact on whole body of a humanoid robot can be very advantageous to work with people in human's environment. In the tasks with environmental contacts, it is important as an interface with the environment to detect pushing, shearing and twist on the whole body of a robot such that it gets to know its current state and what to do next. In this paper, we describe a full body soft tactile sensor suit for a humanoid robot and an algorithm to calculate pushing, shearing, and twist for each sensor unit. These sensors are small muti-axis sensors with urethane structure and they can be placed densely on the body of a humanoid robot. We arranged 347 multi-axis soft tactile sensors on a humanoid robot imitating a human tactile sense to detect contact states. Then, we calculate a deformation vector for each muti-axis soft tactile sensor and detect the three contact states using deformation moment and average of deformation vectors in the contact surface consisting of soft tactile sensors. Finally, we confirmed the validity of the full body tactile suit and contact state detector by experiments of sitting on a wheelchair and passing object between a human and a robot.**

I. Introduction

In this paper, we propose the construction method of full body soft tactile sensor suit of a life sized humanoid robot with multi-axis soft tactile sensor which can detect contact with environment as Fig.1. Moreover, we show an algorithm to detect the contact state of a surface using tactile information from the sensor suit and verify the validity of them through experiments of sitting a on wheelchair and passing object between a human and a robot.

Then, we adopt a multi-axis soft tactile sensor which has sense of three dimensional deformaiton and can be distributed on the whole body of a humanoid robot [1]. It is a sensor we have developed and its structure is shown in Fig.2(a) It detects three dimensional deformation of its urethane exterior by measuring the amount of light from the leds on its base with five receivers on the its ceiling. It is resistant to heat and shock, and easily distributed throughout the body of a robot because it is small and wiring-saved by SMBus. We can also get shear and twist which are difficult to detect by single-axis pressure sensors using multi-axis soft tactile sensors because they can detect three dimensional deformation of their urethane exterior.

Fig. 1. The humanoid robot covered with a soft body exterior with soft tactile sensors and environmental contacts

In previous researches about whole body tactile of a humanoid robot, there are examples in which high-precision multi-axis force sensors are used and in which small single-axis pressure sensors are used.

A representative example of high-precision multi-axis force sensors is whole-body covering tactile interface with six-axis force sensors implemented on TWENDY [2]. Another examples of full body soft plastic foam cover with soft three-axis force sensors implemented on soft freshy body robot macra [3]. However, it is difficult to distribute muti-axis force sensor throughout the body because of the size of the sensor and wiring between the sensors. Moreover, there are problems in terms of mobility and exhaust heat when force sensors are distributed on a humanoid robot [3].

On the other hand, there is a pioneering example of fullbody soft tactile sensor suit using electrically conductive fabric [4]. It is a detachable sensor suit with electrically condactive cloth and thread which is fit for arbitrary shaped humanoid robots. Conformable and scalable tactile sensor skin is an uniaxial pressing tactile sensor which can be distributed throughout the body of a robot [5]. It is implemented on a whole-body motion humanoid robot and it achieved lifting the 30kg object task [6], and roll-over task [7] using tactile information. A care support robot RIBA has a semiconductor tactile sensor on its arms [8], and communication robot Robovie-IV has piezoelectric element pressure sensor on its body [9]. These distributed sensors are able to be placed densely on the whole body of a robot, but their output are uniaxial limited to the pressing directiona compared to multi-axis force sensors.

II. Multi-axis soft tactile sensor for contact detection

A. Calclation of multi-axis soft tactile sensor's deformation

In this paper, we define the deformation of a soft tactile sensor as 3-dimension vector (θ_x, θ_y, dz) like Fig.2(a). θ_x, θ_y is rotation around x, y axis, and dz is displacement of z axis in its local coordinate.

The deformation is calculated by Eq.1, Eq.2, Eq.3. We define $(r_1, r_2, r_3, r_4, r_5)$ as raw output of receiver 1 to 5 in Fig.2(a). $(r_{10}, r_{20}, r_{30}, r_{40}, r_{50})$ is the initial output of receiver 1 to 5.

$$\theta_x = k_x\{(r_2 - r_{20}) - (r_1 - r_{10})\} \tag{1}$$
$$\theta_y = k_y\{(r_4 - r_{40}) - (r_3 - r_{30})\} \tag{2}$$
$$dz = \frac{k_z}{r_5^2} - z_0 \tag{3}$$

Eq.1 and Eq.2 are experimentaly led by relation of r_1, r_2, r_3 and r_4. We concluded by the accuracy evaluation experiment that they can approximate the rotation angles of the sensor ceiling with no practical problems. k_x and k_y are constants led by the output of receivers and the real rotation of the sensor using least-squares method.

Eq.3 is given by the fact that strength of light is inversely propotional to distance from the light source. k_z is a constant and led by Eq.4.

$$k_z = r_{50}^2 z_0 \tag{4}$$

B. Output evaluation of a multi-axis soft tactile sensor

To confirm the detectability of multi-axis soft tactile senosor's deformation, we conducted an evaluation experiment. We fixed a soft tactile sensor on a pedestal, and placed a checkerboard (7×6 grids, 15mm on each side of a grid) on the ceiling of it. We detected position and rotation of the checkerboard using a camera fixed to a height of 160mm from it. The result of the evaluation experiment is TABLEI.

TABLE I
Result of the soft tactile sensor's evaluation

Target	Gradient	Intercept	Standard deviation
θ_x	0.018	-0.21	0.092[rad]
θ_y	0.037	0.33	0.095[rad]
dz	0.98	0.60	0.92[mm]

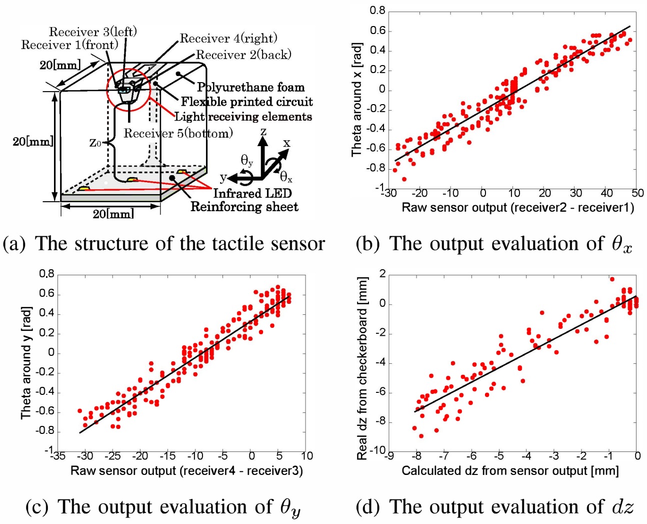

(a) The structure of the tactile sensor
(b) The output evaluation of θ_x
(c) The output evaluation of θ_y
(d) The output evaluation of dz

Fig. 2. The structure and output evaluations of mulit-axis soft tactile sensor

We rotated checkerboard three times around θ_x, θ_y axis in the direction of positive and negative. Fig.2(b) and Fig.2(c) are the result of fitting by least-squares method with raw sensor outputs and real rotation angles in the experiment. From the results, we councluded that there is a positive correlation between the raw sensor outputs and θ_x, θ_y. In this paper, we use the same k_x, k_y ignoring individual differences.

Next, we pushed checkerboard five times to z direction. Fig.2(d) is the result of fitting by by least-squares method with calculated dz from the raw sensor output in accordance with Eq.3 and the real displacement of z direction detected by the camera. We concluded that dz calculated from the sensor output and real displacement of z is matched because the resulting gradient of the experiment was 0.98 although resulting intercept was 0.60.

III. Construction of a dispersively placed full body tactile suit

A. Sensor arrangement based on human's tactile placement

Arrangement of multi-axis soft tactile sensors is an important point which decide the resolution and sensitivity to configure full body soft tactile sensor suit. It is decided by the density, pressure threshold, and max deformation amount of a soft tactile sensor.

When the max deformation amount of a soft tactile sensor is $\pm d_{max}$, the sensor interval should be wider than $2d_{max}$ to avoid interference of adjacent sensors. In this paper, we set the minimum space of sensors as 20mm because the max deformation amount of the sensor we use is 10mm by actual measurement. The human's spatial resolution on body surface is from 35mm to 45mm except hands and toes according to the spatial resolution of human's tactile by S.Weinstein [10]. Therefore, we concluded that minimum spacing between sensors of 20mm is enough to preserve spartial resolution equal to that of a human. In this paper, we took the spacing between sensor on every part of body as shown in TABLEII based on the spatial resolution of human's tactile and minimum spacing between sensors.

The pressure threshold of human is high on abdomen and arms and low on legs according to the sensitivity of tactile sense of a human by S.Weinstein [10]. We measured the hardnes of tactile sensor by a durometer (type CSC2), and decided on the hardness of the tactile sensor on every part of body as TABLEII.

TABLE II
ARRANGEMENT OF THE SOFT TACTILE SENSORS ON HRP-2

Part	Interval	Hardness	Weight	Number
Chest	20[mm]	52.2(Normal)	1.0	56
Upper arms	30[mm]	52.2(Normal)	1.0	21 × 2
Lower arms	25[mm]	52.2(Normal)	1.0	12 × 2
Front of waist	20[mm]	46.4(Soft)	0.5	26
Sides of waist	30[mm]	52.2(Normal)	1.0	6 × 2
Back of body	30[mm]	52.2(Normal)	1.0	30
Hip	30[mm]	71.1(Hard)	1.5	9
Back of thighs	30[mm]	71.1(Hard)	1.5	12 × 2
Legs	30[mm]	52.2(Normal)	1.0	62 × 2
Total				347

B. Implementation of a dispersively placed full body tactile suit

When we implement a fullbody soft tactile sensor suit to a humanoid robot, we should consider that there are planes and curved surfaces on it. Therefore, the implementation method is decided by curvature of the target surface.

In this paper, we directly arranged tactile sensors in a matrix form on the parts consisting of planes such as chest, waist, and hip as given in the left of Fig.3, and wrap soft tactile sensor seats around the parts consisting of curved surfaces such as arms and legs as given in the right of Fig.3.

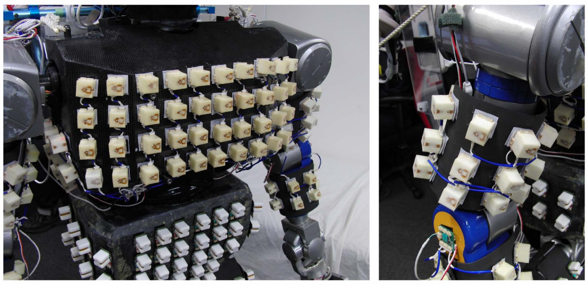

Fig. 3. Implementation of a soft tactile sensor(left: plane, right: curved surface)

IV. CONTACT STATE DETECTION USING FULLBODY SOFT TACTILE SENSOR SUIT

A. Definition of contact state and the algorithm to detect

In this paper, we define push as the state in which a force is perpendicular to the contact surface applied, shear as the state in which a force parallel to the contact surface is applied, and twist as the state in which a moment around the normal of the contact surface is applied. Three states are the contact state. To detect three states, we suggest the following contact state detector.

First, multi-axis soft tactile sensors detect deformation as (θ_x, θ_y, dz). The deformation vector $\boldsymbol{x_d}$ is calculated from the sensor's deformation, and we decide the sensor is in the state of contact with environment or not using the norm of $\boldsymbol{x_d}$. Next, we calculated the deformation moment $\hat{\boldsymbol{M}}_{\boldsymbol{c}}$ and average of $\boldsymbol{x_d}$ as $\boldsymbol{x_{dm}}$ using the index set T consisting of contacting sensors. We can compute the contact state by comparing $\hat{\boldsymbol{M}}_{\boldsymbol{c}}$, $\boldsymbol{x_{dm}}$ and the preset thresholds M_{th}, s_{th}.

B. Tactile information processing from multi-axis soft tactile sensor

1) Calculation of deformation vector: The unit vector of normal direction of the sensor's ceiling $\boldsymbol{e_d} = (e_{dx}, e_{dy}, e_{dz})^T$ can be calculated using the unit vector of z direction of the sensor's local coordinate $\boldsymbol{e_z}$ as Eq.5. $\boldsymbol{R}_{\theta_x}, \boldsymbol{R}_{\theta_y}$ are rotation matrices around x, y axis of the sensor's local coordinate and they can be calculated by θ_x, θ_y. $\boldsymbol{x_d}$ is calculated from $\boldsymbol{e_z}$ as Eq.6 by scalar multiplication so that z-component of $\boldsymbol{x_d}$ is equal to dz.

$$\boldsymbol{e_d} = \boldsymbol{R}_{\theta_y} \boldsymbol{R}_{\theta_x} \boldsymbol{e_z} \tag{5}$$

$$\boldsymbol{x_d} = \frac{dz}{e_{dz}} \boldsymbol{e_d} \tag{6}$$

$\boldsymbol{x_d}$ is perpendicular to ceiling of the sensor and there is a correlation between its norm and the force applied on the ceiling. We define $\boldsymbol{x_d}$ as deformation vector.

When we implement the multi-axis soft tactile sensors to a humanoid robot, the relation between the force applied on the ceiling and the deformaiton vector will change because of the difference of sensor's hardness. Therefore, we weight $\boldsymbol{x_d}$ with w corresponding to the hardness of the sensor as Weight column in TABLEII.

2) Contact detection algorithm: To categorize the multi-axis soft tactile sensors on whole body as contacting to environment or not, we set a relevant threshold d_{th}. If the norm of sensor's deformation vector satisfy $\|\boldsymbol{x_d}\| > d_{th}$, it is considerd in contact.

C. Contact state detection by deformation vector

1) Twist detection algorithm: Every multi-axis soft tactile sensor on whole body has the deformation vector $\boldsymbol{x_d}$ and the posiotion $\boldsymbol{p} = (x, y, z)^T$ and rotation matirx $\boldsymbol{R}$ in the world coordinate.

The center of gravity of contact $\boldsymbol{p_c}$ is calculated as Eq.7 for the index set T consisting of contacting sensors in the contact surface using the norm of deformation vector $\|\boldsymbol{x_d}\|$ as weight.

$$\boldsymbol{p_c} = \frac{\sum_{i \in T} \|\boldsymbol{x_{di}}\| \boldsymbol{p_i}}{\sum_{i \in T} \|\boldsymbol{x_{di}}\|} \tag{7}$$

We define deforamtion moment $\hat{\boldsymbol{M}}_{\boldsymbol{c}}$ using $\boldsymbol{p_c}$ as Eq.8

$$\hat{\boldsymbol{M}}_{\boldsymbol{c}} = \sum_{i \in T} (\boldsymbol{p_i} - \boldsymbol{p_c}) \times (\boldsymbol{R}_i \boldsymbol{x_{di}}) \tag{8}$$

According to the definition of $\boldsymbol{x_d}$, there is a correlation between $\hat{\boldsymbol{M}}_{\boldsymbol{c}}$ and the moment around $\boldsymbol{p_c}$. Therefore, we set a relevant threshold M_{th} and if the normal component of the deformation moment $\hat{M}_{cn}$ satisfies $\|\hat{M}_{cn}\| > M_{th}$, we decide that the contact state is under the state of twist.

2) Shear and push detection algorithm: For the index set T consisting of contacting sensors in the contact surface, we calculate the average deformation vector $\boldsymbol{x_{dm}} = (x_{dm}, y_{dm}, z_{dm})$ as Eq.9. N is the number of multi-axis soft tactile sensors contacting in the contact surface.

$$\boldsymbol{x_{dm}} = \frac{1}{N} \sum_{i \in T} \boldsymbol{x_{di}} \tag{9}$$

We set a relevant threshold s_{th} and if x_{dm} satisfies $\|x_{dm}\| > s_{th}$ or y_{dm} satisfies $\|y_{dm}\| > s_{th}$, we decide that the contact state is under the state of shear. The direction of shear is the larger of $\|x_{dm}\|$ and $\|y_{dm}\|$. Otherwise, we decide that the contact state is under the state of push.

D. Evaluation of contact state detector

To confirm that the contact state detector algorithm can detect the contact state of a contact surface, we experimented contact state detection on the testbed in which 16 multi-axis soft tactile sensors are placed at intervals of 20mm. Live-action part in the left of figure is the state of experiment, and the cubes in model part show the positon and state of the sensors. Detected contact state is showed as the color of sensors. The black arrows on the models are the deformation vectors, the circular arrow on the model view is the deformation moment and the straight arrow on the model view is the estimated direction of the average deformation vector's component according to Subsection IV-C. The graph in the upper right of figure takes the average deformation vector $\boldsymbol{x_{dm}} = (x_{dm}, y_{dm}, z_{dm})$ as the vertical axis and the time as the horizonal axis. The graph in the lower right of figure takes normal component of deformation moment $\hat{M}_{cn}$ as the vertical axis and the time as the horizonal axis.

In this experiment, we defined 16 multi-axis soft tactile sensors in the testbed as a contact surface, and set $d_{th} = 1.0$, $M_{th} =$ 600.0, s_{th} =1.5. Fig.4(a) to Fig.4(d) shows detected contact state and sensor output when we gave x shear, y shear, push, and twist.

Fig.4(a) and Fig.4(b) show the state when we gave x and y shear to the testbed. It is seen that $\hat{M}_{cn}$ satisfies $\|\hat{M}_{cn}\| < M_{th}$, x_{dm} and y_{dm} satisfy $\|x_{dm}\|, \|y_{dm}\| > s_{th}$ in both figures. It is also seen that x_{dm} and y_{dm} satisfy $\|x_{dm}\| > \|y_{dm}\|$ in Fig.4(a) and $|y_{dm}\| > \|x_{dm}\|$ in Fig.4(b). Fig.4(c) shows the state when we gave push to the testbed. It is seen that $\hat{M}_{cn}$ satisfies $\|\hat{M}_{cn}\| < M_{th}$, x_{dm} and y_{dm} satisfy $\|x_{dm}\|, \|y_{dm}\| < s_{th}$. This means that the sensor outputs satisfies conditions of the state of push. Fig.4(d) shows the state when we gave twist to the testbed. It is seen that $\hat{M}_{cn}$ satisfies $\|\hat{M}_{cn}\| > M_{th}$, x_{dm} and the sensor outputs satisfies conditions of the state of twist.

According to the experiment, it was shown that we can detect the (x, y, z) deformation and rotation around the normal of the contact surface using suggested contact state detector with relevant thresholds.

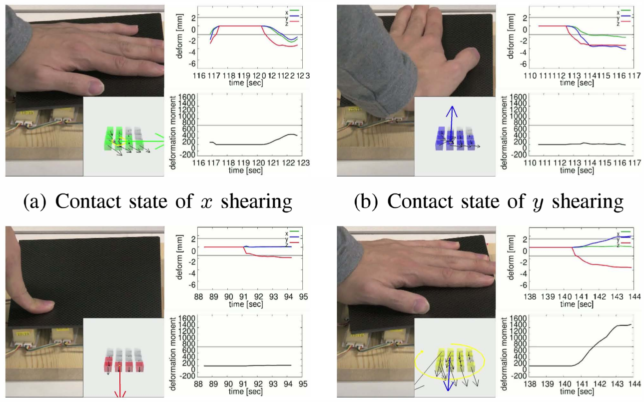

(a) Contact state of x shearing (b) Contact state of y shearing

(c) Contact state of z pushing (d) Contact state of twist

Fig. 4. Contact state estimation in a 4x4 testbed

V. Environmental Contact Experiment with Contact State Detection

We performed environmental contact experiments between a human and the humanoid robot HRP-2 [11] with full body soft tactile sensor suit using the hardware configuration and contact detection algorithm mentioned in Section III and Section IV. The figures of experiments follow the format of Fig.4. In this section, we divided the body of the humanoid robot into 21 parts, namely front body, left and right side of body, back, hip, and every side of legs and arms. We take each of them as a contact surface.

A. Sitting on a wheelchair with pushing

We conducted the experiment in which a humanoid robot sat on a wheelchair detecting its seat and backrest by whole body tactile sensors as the example of a proactive environmental contact. Fig.5 shows results. We set $d_{th} =$ 1.0, $M_{th} =$ 1000.0, $s_{th} =$ 1.5 in this experiment. We used the surface which is a conbination of the hip and the back of the thighs and back of the body as contact surfaces in this experiment, so we show data from the hip and back of thighs as solid lines and from back of the body as dotted lines.

The humanoid robot could recognize the seat and backrest of wheelchair by pushing on the back of the body and the thighs which are detected as merely increasing z_{dm} on each contact surfaces when it sit down. It could sit stable on the wheelchair without slipping down maintaining the contact to its seat and backrest using tactile sensors.

B. Passing objects action with a response to contact

We made the humanoid robot receive and pass a box which size is 500mm $\times$ 500mm $\times$ 70mm as example of a rectangular shaped rigid object, three paper tubes which radius is 35mm and height is 1200mm as example of a cylindrical shaped rigid object, and a doll which length is 1200mm and width is 300mm as complex shaped flexible

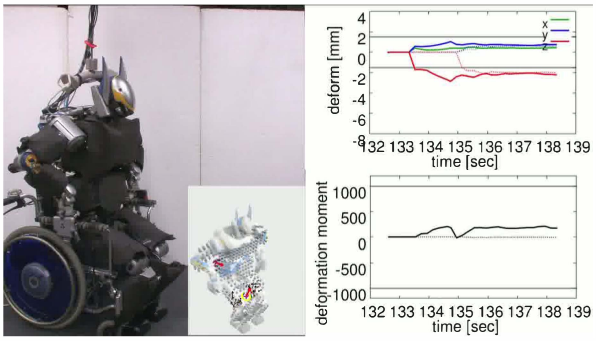

Fig. 5. Detect the seat and backrest of a wheelchair and sitting on it

object. We applied the force control at the hands as their reaction forces ware 0N.

1) Holding objects in arms with pushing and twist: We conducted an experiment in which a human gives an object to a robot and the robot gives it back to the human as the example of task achivement using push and twist detection. The robot holds the object in its arms when it detects the state of push in its front body, and it detects the state of twist in its front body and releases the object when a human rotates the object held by it.

Fig.6 shows result of the experiment where a human gives a box to the humanoid robot with full body soft tactile sensor suit. In this experiment, we set d_{th} = 1.0, M_{th} = 150.0, s_{th} = 1.5. The humanoid robot detected the state of push because only z_{dm} increased when a human pressed a box to its front body and held the box in its arms in the left of Fig.6. Next, the humanoid robot detected the state of twist because $\hat{M}_{cn}$ satisfies $\|\hat{M}_{cn}\| < M_{th}$ when a human rotated the box and release it in the right of Fig.6. Therefore, we concluded that the robot was able to detect the state of push and twist by the proposed method. We also conducted an experiment to show that the robot could detect state of push and twist when it held flexible and cylindrical shaped object in its arms. The results are showed in Fig.7. We set d_{th} = 1.0, M_{th} = 200.0, s_{th} = 1.5 in this experiment.

2) Putting objects between arms with push and shear: We conducted an experiment where a robot holds a doll and paper tubes between its side as the example of task achivement using twist detection. Fig.8 and Fig.9 show the results. We used the left side of the body and the right side of the left arm as contact surfaces in this experiment, so we show data from left side of the body as solid lines and from right side of the left arm as dotted lines.

The robot holds the object between its side when it detects the state of push in the left side of its body, and it detects the state of shear in its side and release the object when a human moves the object held by it. The optimal angles of shoulder and elbow joint depend on the object when a robot holds it under the arm. The robot can hold it under the arm in the appropriate strength without hard-corded joint angles by detecting contact states of side of its body and inner arm. It recognizes that someone attempts to receive the holding object when it detects the state of shear in the left side of its body and the right side of its left arm and release it.

From left of Fig.8 and Fig.9, it is found that the humanoid robot detected the state of push because only z_{dm} increased when a human pressed a doll and paper tubes to the left side of its body. Moreover, it is seen that the humanoid robot detected the state of shear because y_{dm} satisfies $\|y_{dm}\| > s_{th}$ when a human moves the object it holds and release it in the right of Fig.8 and Fig.9. Although it is seen that the humanoid robot detected the state of twist from the graph of deformation moment in Fig.9 before it detected the state of shear, it is due to the rotation caused by the paper tubes in the process until their pose became stable.

VI. Conclusion

In this paper, we showed a construction method as well as the validity of a soft tactile sensor suit for a humanoid robot. We could detect three contact states, which are pushing, shearing and twist, using deformation of the sensors in the contact surface. We proposed following steps:

- We configured a soft tactile sensor suit by arranging 347 multi-axis soft tactile sensors on a humanoid robot imitating a human tactile sense. We coped with both dense arrangement and multi-axis output by small and wiring-saved multi-axis soft tactile sensors.
- We defined the deformation vector, which is calculated from deformation of the sensor so it could detect pushing, and yet more challenging shearing and twist.
- We assessed the validity of the soft tactile sensor suit and contact state detector by environmental contact experiments The robot could detect the contact states and could successfullly sit on a wheelchair and pass objects using its whole body.

A Humanoid robot can detect three contact states by implementing the full body soft tactile sensor suit, and perfoms carrying action and interaction with people, which is more difficult to achive for robots without tactile to do. Therefore, we can use tactile interface in cooperative behaviors of human and robot such as carrying objects. This can help introducing humanoid robots to human's living space.

References

[1] A. Kadowaki, T. Yoshikai, M. Hayashi, and M. Inaba. Development of soft sensor exterior embedded with multi-axis deformable tactile sensor system. In *Robot and Human Interactive Communication, 2009. RO-MAN 2009. The 18th IEEE International Symposium on*, pages 1093 –1098, 27 2009-oct. 2 2009.

[2] H. Iwata and S. Sugano. Whole-body covering tactile interface for human robot coordination. In *Robotics and Automation, 2002. Proceedings. ICRA '02. IEEE International Conference on*, volume 4, pages 3818 – 3824 vol.4, 2002.

[3] M. Hayashi, T. Sagisaka, Y. Ishizaka, T. Yoshikai, and M. Inaba. Development of functional whole-body flesh with distributed three-axis force sensors to enable close interaction by humanoids. In *Intelligent Robots and Systems, 2007. IROS 2007. IEEE/RSJ International Conference on*, pages 3610 –3615, 29 2007-nov. 2 2007.

[4] M. Inaba, Y. Hoshino, K. Nagasaka, T. Ninomiya, S. Kagami, and H. Inoue. A full-body tactile sensor suit using electrically conductive fabric and strings. In *Intelligent Robots and Systems '96, IROS 96, Proceedings of the 1996 IEEE/RSJ International Conference on*, volume 2, pages 450 –457 vol.2, nov 1996.

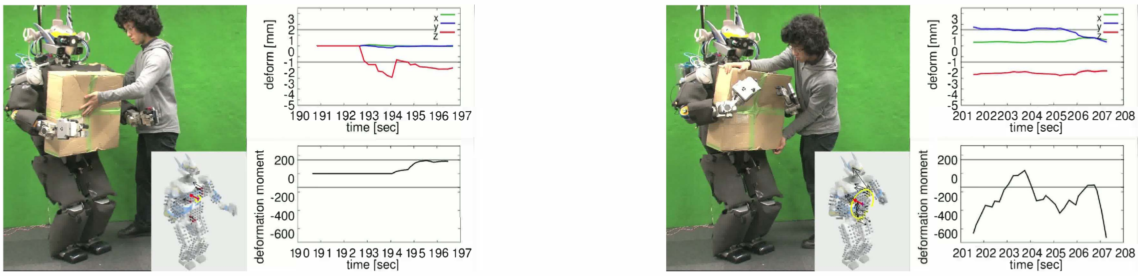

Fig. 6. Left: detect contact of a box by tactile sensors on chest, right: detect rotation of a box by tactile sensors on chest

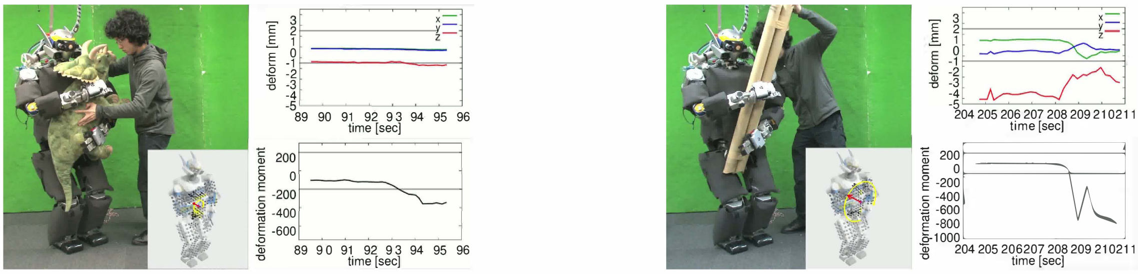

Fig. 7. Left: detect rotation of a doll by tactile sensors on chest, right: detect rotation of sticks by tactile sensors on chest

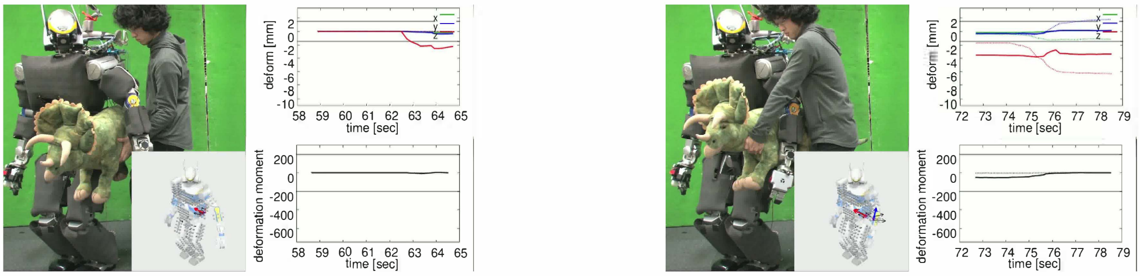

Fig. 8. Left: detect contact of a doll by tactile sensors on left side, right: detect y deformation of a doll by tactile sensors on left inner arm

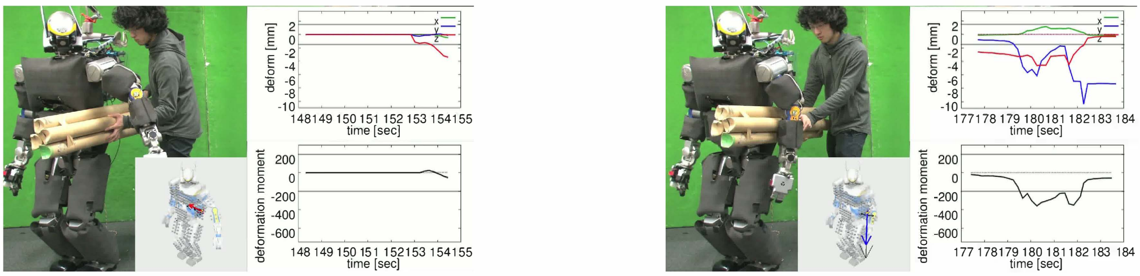

Fig. 9. Left: detect contact of sticks by tactile sensors on left side, right: detect y deformation of sticks by tactile sensors on left side

[5] Yoshiyuki Ohmura, Yasuo Kuniyoshi, and Akihiko Nagakubo. Conformable and scalable tactile sensor skin for curved surfaces. In *Proc. IEEE Int. Conf. on Robotics and Automation*, pages 1348–1353, 2006.

[6] Y. Ohmura and Y. Kuniyoshi. Humanoid robot which can lift a 30kg box by whole body contact and tactile feedback. In *Intelligent Robots and Systems, 2007. IROS 2007. IEEE/RSJ International Conference on*, pages 1136 –1141, 29 2007-nov. 2 2007.

[7] Yasuo Kuniyoshi, Yoshiyuki Ohmura, and Akihiko Nagakubo. Whole body haptics for augmented humanoid task capabilities. In *ISRR*, pages 61–73, 2007.

[8] T.Mukai, S.Hirano, H.Nakashima, Y.Kato, Y.Sakaida, S.Guo, and S.Hosoe. Development of a nursing-care assistant robot riba that can lift a human in its arms. *Proceedings of the IEEE/RSJ 2010 International Conference on Intelligent Robots and Systems*, pages 5996–6001, 2010.

[9] N. Mitsunaga, T. Miyashita, H. Ishiguro, K. Kogure, and N. Hagita. Robovie-iv: A communication robot interacting with people daily in an office. In *Intelligent Robots and Systems, 2006 IEEE/RSJ International Conference on*, pages 5066 –5072, oct. 2006.

[10] S.Weinstein. Intensive and extensive aspects of tactile sensitivity as a function of body part, sex, and laterality. *the First Int' l symp. on the Skin Senses*, pages 195–222, 1968.

[11] K. Kaneko, F. Kanehiro, S. Kajita, H. Hirukawa, T. Kawasaki, M. Hirata, K. Akachi, and T. Isozumi. Humanoid robot hrp-2. In *Robotics and Automation, 2004. Proceedings. ICRA '04. 2004 IEEE International Conference on*, volume 2, pages 1083 – 1090 Vol.2, 26-may 1, 2004.